The influence of crustal strength on rift geometry and development – Insights from 3D numerical modelling

Thomas B. Phillips[1], John B. Naliboff[2], Ken J. W. McCaffrey[1], Sophie Pan[3], Jeroen van Hunen[1]

[1] Department of Earth Science, Durham University, Science Labs, Durham, DH13LE, UK
[2]Department of Earth and Environmental Science, New Mexico Institute of Mining and Technology, Socorro, New Mexico, USA
[3] Basins Research Group (BRG), Imperial College, London, SW72BP, UK

Abstract

The lateral distribution of strength within the crust is highly variable. When subject to extension, lithologically and rheologically distinct areas of crust manifest strain differently, influencing the structural style, geometry and evolution of the associated rift system. Here, we use 3D thermo-mechanical models of continental extension to explore how pre-rift upper crustal strength variations influence rift physiography. We model a 500x500x100 km volume containing 125 km wide domains of mechanically 'Strong' and 'Weak' upper crust along with two reference domains. Crustal strength is represented by varying the initial strength of 5 km^3 blocks. Extension is oriented parallel to the domain boundaries such that each domain is subject to the same 5 mm/yr extension rate. Our modelling results show that strain initially localises in the Weak domain, producing a well-developed fault network, whilst little to no localisation occurs in the Strong domain, which is characterised by uniform strain. We find that although faults in the Weak domain are initially inhibited at the terrane boundaries, they eventually propagate through and 'seed' faults in the relatively stronger adjacent domains. We show characteristic structural styles associated with 'strong' and 'weak' crust and relate our observations to rift systems developed across laterally heterogeneous crust worldwide, such as the Great South Basin, NZ, and the Tanganyika rift, East Africa.

1 Introduction

Continental rifts form atop a mosaic of crustal units, including cratons, mobile orogenic belts, magmatic terranes, and sedimentary sequences, amalgamated through multiple tectonic events. Each crustal unit has distinct lithological properties and a suite of pre-existing heterogeneities acquired through their unique tectonic evolution (e.g. Thomas, 2006). These crustal units manifest strain differently when subject to extension, influencing the development of rift systems.

The relative bulk strength of a crustal volume is dependent on its lithological and rheological properties, and the presence of any heterogeneities within it, which reduce overall bulk strength (e.g. Sutton and Watson, 1986; Holdsworth et al., 2001). Strong crustal volumes may include rheologically strong cratons or relatively homogeneous granitic batholiths (e.g. Thomas, 2019; Howell et al., 2020); whilst weak volumes encompass rheologically weak sedimentary sequences and areas with pervasive heterogeneities, such as older rift systems (Cowie et al., 2005; Henza et al., 2011; Naliboff and Buiter, 2015), or orogenic belts surrounding cratons (Daly et al., 1989). Strong crust proves resistant to extension, with strain localising into adjacent weaker areas (e.g. Beniest et al., 2017; Lang et al., 2020). However, when extension occurs at a high angle to the boundaries between crustal volumes, as in the Great South Basin, New Zealand (Figure 1a) (e.g. Phillips and McCaffrey, 2019; Sahoo et al., 2020), and the Lake Tanganyika Rift, East Africa (Figure 1b) (Wright et al., 2020), each volume, regardless of strength, experiences is subject to the same stress and undergoes extension, offering insights into how strain is accommodated across areas of different strength. In addition, boundaries between crustal volumes may reactivate or segment rift systems depending on their orientation, further influencing rift physiography (Doré et al., 1997; Fossen et al., 2016; Vasconcelos et al., 2019). The structural style and evolution of rift systems reflects this geologically and rheologically complex crustal substrate, yet how strain is manifest across and between crust of varying strength, remains relatively unknown.

In this study, we use 3D thermo-mechanical simulations of continental rifting to investigate how rift physiography varies across crustal units of varying initial strength. We extend a 500x500x100 km region consisting of four 125-km wide domains, assigned different crustal strengths and oriented parallel to the extension direction (Figure 1c). The relative strengths of each domain is represented by randomly varying the initial brittle strength (parameterized through plastic strain softening) between 5 km^3 'Unit Blocks', with weaker domains containing weaker Unit Blocks and a greater contrast between blocks. Our modelling results highlight how crustal strength and heterogeneities related to prior deformation influence strain localisation and rift physiography. We document characteristic structural styles associated with Strong and Weak crust, and highlight how faults developed in the weaker domains influence those developing in relatively stronger material across domain boundaries.

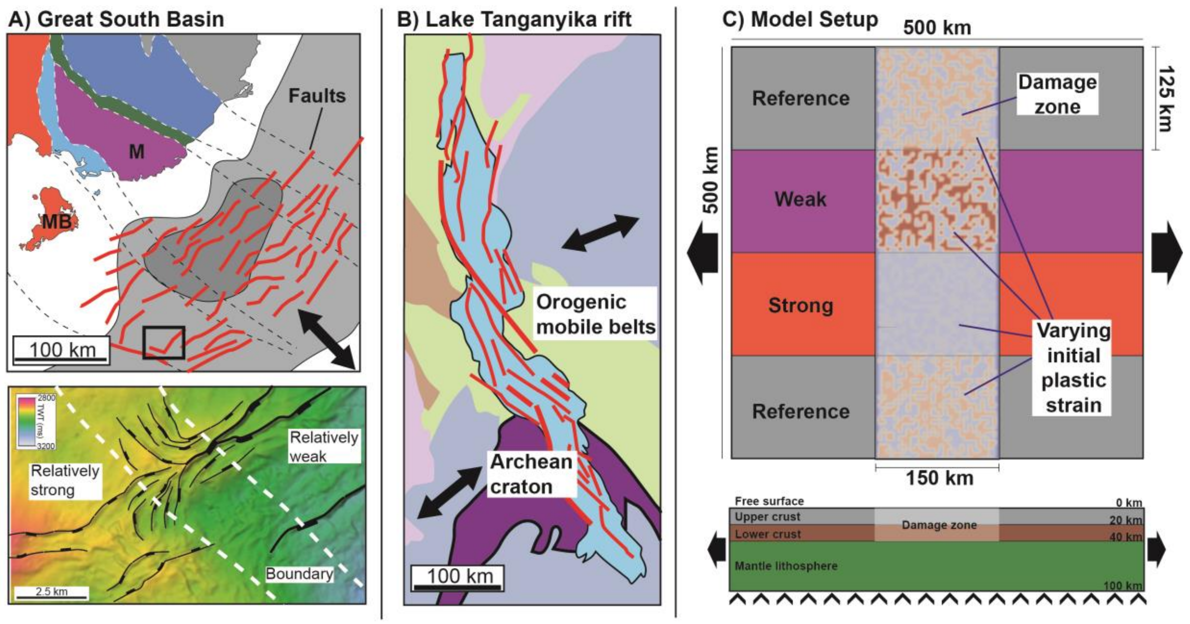

Figure 1 – A) Top – Great south Basin, New Zealand, developed across an assortment of basement terranes including the Median Batholith (MB) and Murihiku forearc sedimentary basin (M). Faults after Sahoo et al., (2020) and Phillips and McCaffrey, (2019). Bottom – TWT structural map showing how faults terminate at a boundary with stronger material (granitic body within the Median Batholith). After Phillips and McCaffrey, 2019. B) Map of the Lake Tanganyika rift, East Africa, traversing orogenic mobile belts and an Archean craton. After Wright et al., (2020). Black arrows indicate extension

direction. C) Initial numerical model setup. Initial Plastic Strain is added across the central 150 km of the model, varying between four domains of varying strength.

2 Numerical approach

2.1 Modelling design and geometry

We model the 3D thermo-mechanical evolution of extending continental lithosphere using the mantle convection and lithospheric dynamics ASPECT (Kronbichler et al. 2012; Heister et al. 2017; Glerum et al., 2018; Naliboff et al., 2020). The simulations span 500x500x100 km and fixed outward velocities drive extension at a constant rate of 5 mm/yr (Figure 1c). Inflow along the lower boundary balances outflow, while a stress free upper boundary allows the development of topography (Rose et al., 2017).

The initial lithospheric structure contains distinct lithologies with thermodynamic and rheological properties characteristic of the upper crust (0-20 km depth), lower crust (20-40 km depth), and mantle lithosphere (40-100 km depth) (Figure 1c). The rheological structure follows a visco-plastic constitutive relationship, which captures both brittle (plastic) and ductile (viscous) deformation processes observed within rifts and rifted margins. Coupling brittle strain softening of cohesion and the internal angle of friction with randomized initial plastic strain (IPS) enables the formation of distributed normal fault networks (Naliboff et al., 2017; Naliboff et al., 2020; Duclaux et al., 2020). We use variable distributions of the IPS along the model length to define upper crustal volumes of differing strength (e.g., distinct geologic terranes), with the cohesion and angle of internal friction decreasing linearly between defined IPS values (e.g., strain softening interval).

The initial resolution throughout the model is set to 5 km, and refined to 1.25 km in the upper 20 km (i.e. upper crust) across the central 150 km of the model. This approach enables a relatively high resolution in the region of interest (upper crust), while producing ‘natural’ boundary conditions at its base.

2.2 Upper crustal domain strength

We define four 125 km wide upper crustal domains, oriented parallel to the extension direction, to replicate different strengths. From top to bottom, the domains are assigned Reference, Weak, Strong, and Reference strengths (Figure 1c). We assign IPS values to 5 km^3 blocks, termed Unit Blocks, in the Upper Crust across the central 150 km of the model, termed the Damage zone.

IPS values were randomly assigned to unit blocks in a binary fashion, such that a block either has the minimum or maximum value specific to that strength. The initial cohesion (20 MPa) and internal angle of friction (30^{o}), decrease by a factor of 4 between plastic strain values of 0.5-1.5. We assign default IPS values of 0.5 to Unit Blocks within the Damage zone, with zero IPS outside of the zone. The Reference domains comprise Unit blocks with IPS of 0.5 or 1, producing a potential contrast of 0.5 between blocks. The Weak domain has a 1.0 IPS contrast between unit Blocks (0.5-1.5), whilst the Strong domain has a 0.1 IPS contrast. Weaker domains contain Unit blocks with higher IPS values and greater potential IPS contrasts between adjacent blocks (Figure 1c).

We explored a wide range of IPS values and combinations within each domain as well as the rate of strain weakening for different models, details of which can be found in the supplementary material.

3 Model results

Each domain is subject to the same 5 mm/yr extension rate; however, how strain localises across the model varies markedly between domains and across their boundaries.

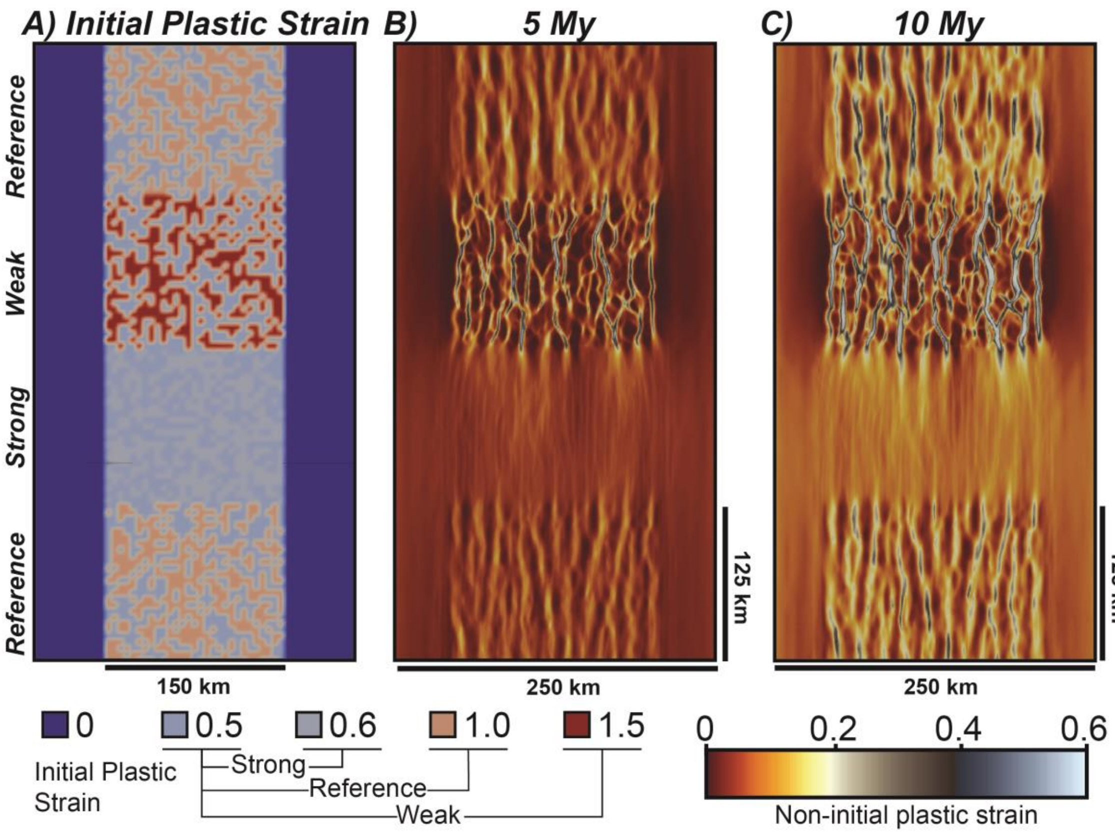

Figure 2 – Top view model results. A) Initial Plastic strain in the model prior to extension, delineating the different crustal domains. B, C) Accumulated (non-initial) plastic strain at 5 (A) and 10 My (B), highlighting the different strucutral styles between domains. Non-uniform colour bar chosen to highlight strain in both the Weak and Strong domains.

3.1 Weak Domain

The weak domain is characterised by a high-strain, widely-spaced fault network, separated by low-strain shadows (Figure 2). Per-fault strain is ~0.5-1 and fault spacing ~5-10 km. Faults are largely perpendicular to the extension direction, although some variation occurs due to lateral fault linkages and interactions (Figure 2). The fault network is established early and remains fixed throughout the model run (See Fault A on Figure 3).

3.2 Strong Domain

The Strong domain is characterised by uniform strain with little to no localisation onto faults. Wide zones of increased strain start to develop towards the end of the run, adjacent to the domain boundaries (Figure 2a, 3b). The total accumulated strain across the Strong Domain is less (~18 across the transect) than that of the Weak Domain (~22) (Figure 3c), suggesting less first-order focussing of strain into the Damage Zone.

3.3 Reference Domains

Both Reference domains display localised faults, albeit with a lower fault spacing (~3-5 km) and per-fault strain (~0.5) than the Weak Domain (Figure 3). Faults are typically linear with a uniform spacing, and display some transient properties throughout the model run (Figure 2). Localisation onto faults occurs earlier in the top Reference domain, adjacent to the Weak domain, than in the bottom Reference domain, which is adjacent to the Strong Domain. The bottom Reference domain has a decreased per-fault strain, fault-spacing and cumulative strain compared to the top (Figure 3c).

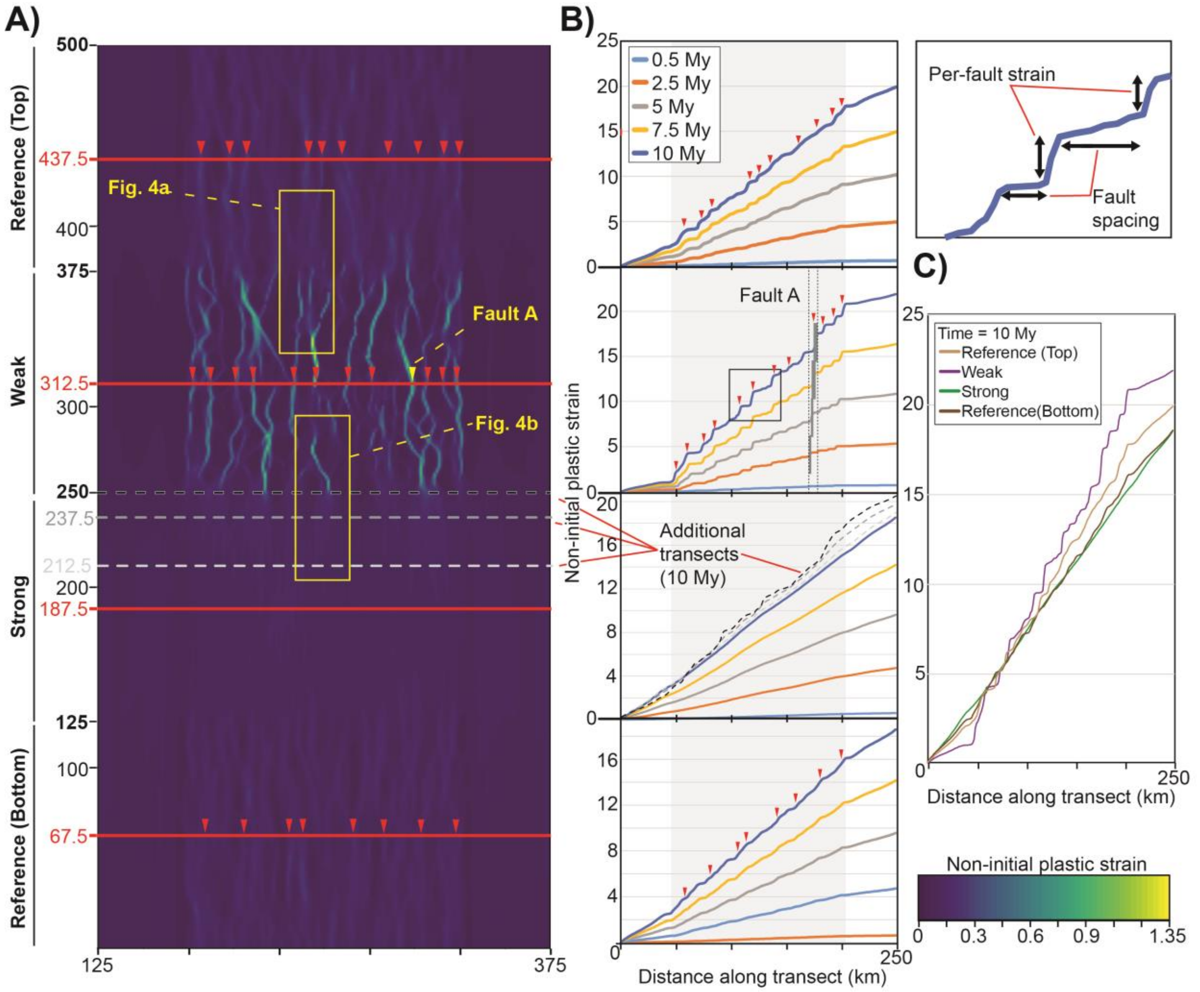

Figure 3 – A) Top view model geometry at 10 My. B) Cumulative strain transects for each domain (see red lines on A), taken at various timesteps throughout the model run. Note the migration of Fault A through time in the Weak domain. C) Comparison of cumulative strain across each domain, note the relatively uniform strain recorded in the Strong domain, compared to the stepped profile of the Weak domain.

3.4 Strain localisation across domain boundaries

We analyse fault geometry across the Reference-Weak and Weak-Strong domain boundaries (Figure 4). Strain is more localised in the Weak compared to the Reference domain, with the latter having a higher background strain (i.e. more distributed) (Figure 4a). The Weak-Reference boundary is characterised by a ~10 km zone of diffuse strain (Figure 4a). To the south, highly localised faults in the Weak domain are inhibited at and dissipate towards the Strong domain boundary (Figure 4b). Broad zones of elevated strain characterise the boundary-proximal Strong domain and persist up to 25 km away from the boundary (Figure 3b, 4b).

This transition from localised to diffuse strain across domain boundaries demonstrates a ‘seeding’ effect of faults in stronger domains by those in weaker domains (Figure 4). Established faults propagate into adjacent stronger domains, initially as broad zones of elevated strain that become increasingly localised. Faults in the top Reference domain are partially ‘seeded’ by those in the adjacent Weak domain. However, as the bottom Reference domain is weaker than the adjacent Strong domain, faults here are not seeded and initiate independently, accounting for the differences between the Reference domains (Figure 3). In turn, faults in the bottom Reference domain may, along with faults in the Weak domain, seed faults in the Strong Domain (Figure 4b).

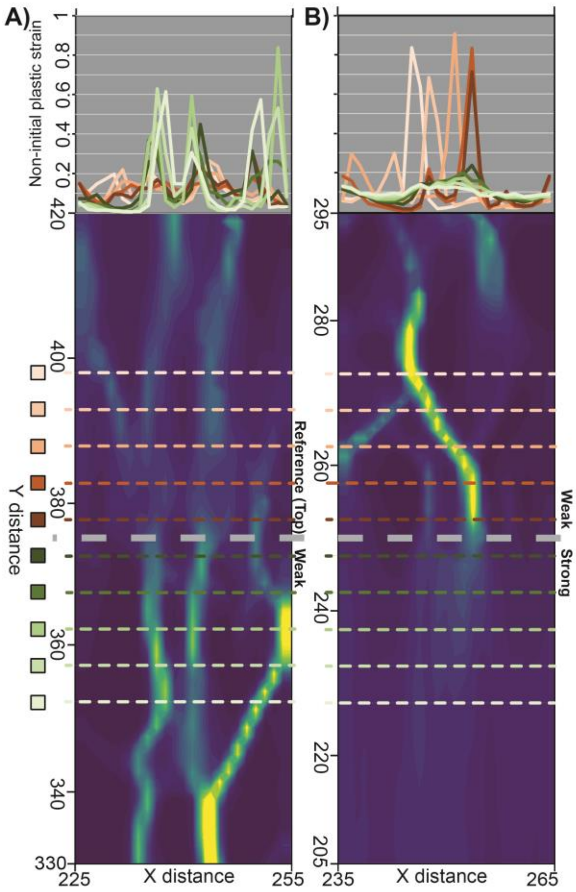

Figure 4 – Closeup map-view of domains boundaries with transects showing where strain is localised.. See figure 3a for locations. A) Boundary between the Reference and Weak domains. B) Weak-Strong domain boundary. Note the the broad zone of elevated strain emanating from the Weak and extending into the Strong domain.

4 Comparison to natural rift systems

Our models showcase an idealised scenario where rifting occurs parallel to crustal terranes of varying strength separated by vertical boundaries. Here, we relate key first-order observations from our models to rift systems globally.

Rift structural style varies markedly between domains. The Weak domain is characterised by relatively widely-spaced, high-strain faults and the Strong domain by a lack of localisation and distributed, uniform strain (Figure 2, 3). Strong bodies, such as granites, typically resist strain localisation, as exemplified by their role as ‘blocks’ in the ‘block and basin’ geometry of UK Carboniferous rift systems (Fraser and Gawthorpe, 1990; Howell et al., 2020), and the Sierra Nevada Batholith in the USA, which buffers extension in the Basin and Range (Ryan et al., 2020). Although it resists extension, the margin of the Sierra Nevada batholith is characterised by low-magnitude seismicity. We hypothesise that, across geological time, this low seismicity may be similar to our observations in the Strong domain, with the uniform strain approximating infinitesimally small and closely-spaced faults, concurring with the decrease in per-fault strain and spacing with increasing strength (Figure 3).

Strain localisation occurs diachronously across the model, first in the Weak domain, and last in the Strong domain (Figure 3b). Rifting in the Great South Basin, New Zealand, initiates in the sedimentary/volcaniclastic Murihiku and Brook Street Terranes prior to the granitic Median Batholith (Figure 1a) (Sahoo et al., 2020); and extension in the Tanganyika rift rapidly localises onto border faults where the rift traverses Proterozoic mobile belts, but remains distributed across the cratonic Bangwelu Block (Figure 1b) (Wright et al., 2020). Here, the mobile belts host prominent fabrics, similar to the large IPS contrasts in the Weak domain (Figure 2a), allowing strain to localise. In contrast, the cratonic Bangwelu Block hosts only weakly-developed fabrics, analogous to the small IPS contrasts present between

Unit blocks in the Strong domain, inhibiting strain localisation (Wright et al., 2020). Similar observations have been made from analog modelling studies, which show more distributed (uniform) deformation in areas of stronger basement (Samsu et al., 2021).

On first consideration, rifts such as the Labrador Sea appears to contradict our model results and the geological observations described above. Here, continental rifting and breakup proceeded rapidly in the strong North Atlantic Craton and was suppressed in the weaker orogenic belts, in contrast to our model observations (Gouiza and Naliboff, 2020; Peace et al., 2017). However, we note that numerous onshore heterogeneities identified in the strong North Atlantic Craton onshore extend beneath the Labrador Sea (Peace et al., 2017; Wilson et al., 2006). We suggest these heterogeneities represent weaknesses that partition the craton, forming isolated 'islands' of strength separated by weaknesses. As such, our homogeneous model Strong domain represents a simplification. Whilst the strong 'islands' resist extension, as in our model Strong domain (Figure 2), strain may rapidly localise along the surrounding weaker heterogeneities. As strain continues to localise, faults may propagate through the thick brittle upper crust, negating any upper crustal strength variation, and accelerating continental breakup (Gouiza and Naliboff, 2020).

We find that faults are inhibited at boundaries with adjacent, stronger domains, before potentially propagating through (Figure 4). In the Great South Basin, faults commonly align with the boundary or segment and terminate against stronger areas (Figure 1a) (Phillips and McCaffrey, 2019; Sahoo et al., 2020). Our model observations show that as faults are initially arrested at the boundaries, diffuse areas of strain form in the stronger area, potentially analogous to damage zones in nature (Figure 3b). Once the stronger domain is sufficiently weakened by these broad zones, strain may localise and 'seed' faults in the stronger domains (Figure 3a).

As well as upper crustal structure, mantle heterogeneities also influence rift development (e.g. Heron et al., 2019). Whilst we do not incorporate any brittle heterogeneities in the mantle lithosphere, we suggest that mantle heterogeneities influence rift location and that of eventual breakup, similar to the role played by the damage zone in our models (Figure 1c). Whilst these deeper structures may control rift location, we suggest that rift structural style and physiography is primarily controlled by upper crustal properties and structures.

Our modelling highlights how upper crustal strength distributions influence rift geometry and evolution. We document characteristic structural styles associated with strong and weak crust and examine how strain is manifest across boundaries between areas of different strength. We relate our findings to multiple rift systems globally, offering additional insights into their evolution and to fundamental continental rifting processes.

References

Beniest, A., Willingshofer, E., Sokoutis, D., & Sassi, W. (2018). Extending continental lithosphere with lateral strength variations: effects on deformation localization and margin geometries. Frontiers in Earth Science, 6, 148. https://doi.org/10.3389/feart.2018.00148

Cowie, P. A., Underhill, J. R., Behn, M. D., Lin, J., & Gill, C. E. (2005). Spatio-temporal evolution of strain accumulation derived from multi-scale observations of Late Jurassic rifting in the northern North Sea: A critical test of models for lithospheric extension. Earth and Planetary Science Letters, 234(3-4), 401-419. https://doi.org/10.1016/j.epsl.2005.01.039

Daly, M. C., Chorowicz, J., & Fairhead, J. D. (1989). Rift basin evolution in Africa: the influence of reactivated steep basement shear zones. Geological Society, London, Special Publications, 44(1), 309-334. https://doi.org/10.1144/GSL.SP.1989.044.01.17

Doré, A. G., Lundin, E. R., Fichler, C., & Olesen, O. (1997). Patterns of basement structure and reactivation along the NE Atlantic margin. Journal of the Geological Society, 154(1), 85-92. https://doi.org/10.1144/gsjgs.154.1.0085

Duclaux, G., Huismans, R. S., & May, D. A. (2020). Rotation, narrowing, and preferential reactivation of brittle structures during oblique rifting. Earth and Planetary Science Letters, 531, 115952. https://doi.org/10.1016/j.epsl.2019.115952

Fossen, H., Khani, H. F., Faleide, J. I., Ksienzyk, A. K., & Dunlap, W. J. (2017). Post-Caledonian extension in the West Norway–northern North Sea region: the role of structural inheritance. Geological Society, London, Special Publications, 439(1), 465-486. https://doi.org/10.1144/SP439.6

Fraser, A. J., & Gawthorpe, R. L. (1990). Tectono-stratigraphic development and hydrocarbon habitat of the Carboniferous in northern England. Geological Society, London, Special Publications, 55(1), 49-86. https://doi.org/10.1144/GSL.SP.1990.055.01.03

Glerum, A., Thieulot, C., Fraters, M., Blom, C., & Spakman, W. (2018). Nonlinear viscoplasticity in ASPECT: Benchmarking and applications to subduction. Solid Earth, 9(2), 267–294. https://doi.org/10.5194/se-9-267-2018

Gouiza, M., & Naliboff, J. (2020). Rheological inheritance controls the formation of segmented rifted margins in cratonic lithosphere. Earth and Space Science Open Archive ESSOAr. https://doi.org/10.1002/essoar.10504071.1

Heister, T., Dannberg, J., Gassmöller, R., & Bangerth, W. (2017). High accuracy mantle convection simulation through modern numerical methods–II: realistic models and problems. Geophysical Journal International, 210(2), 833-851. https://doi.org/10.1093/gji/ggx195

Heron, P. J., Peace, A. L., McCaffrey, K. J., Welford, J. K., Wilson, R., van Hunen, J., & Pysklywec, R. N. (2019). Segmentation of rifts through structural inheritance: Creation of the Davis Strait. Tectonics, 38(7), 2411-2430.

Henza, A. A., Withjack, M. O., & Schlische, R. W. (2011). How do the properties of a pre-existing normal-fault population influence fault development during a subsequent phase of extension?. Journal of Structural Geology, 33(9), 1312-1324. https://doi.org/10.1016/j.jsg.2011.06.010

Holdsworth, R. E., Handa, M., Miller, J. A., & Buick, I. S. (2001). Continental reactivation and reworking: an introduction. Geological Society, London, Special Publications, 184(1), 1-12. https://doi.org/10.1144/GSL.SP.2001.184.01.01

Howell, L., Egan, S., Leslie, G., Clarke, S., Mitten, A., & Pringle, J. (2020). The influence of low-density granite bodies on extensional basins. Geology Today, 36(1), 22-26. https://doi.org/10.1111/gto.12297

Kronbichler, M., Heister, T., & Bangerth, W. (2012). High accuracy mantle convection simulation through modern numerical methods. Geophysical Journal International, 191(1), 12-29. https://doi.org/10.1111/j.1365-246X.2012.05609.x

Lang, G., ten Brink, U. S., Hutchinson, D. R., Mountain, G. S., & Schattner, U. (2020). The Role of Premagmatic Rifting in Shaping a Volcanic Continental Margin: An Example From the Eastern North American Margin. Journal of Geophysical Research: Solid Earth, 125(11). https://doi.org/10.1029/2020JB019576

Naliboff, J., & Buiter, S. J. (2015). Rift reactivation and migration during multiphase extension. Earth and Planetary Science Letters, 421, 58-67. https://doi.org/10.1016/j.epsl.2015.03.050

Naliboff, J. B., Glerum, A., Brune, S., Péron-Pinvidic, G., & Wrona, T. (2020). Development of 3-D rift heterogeneity through fault network evolution. Geophysical Research Letters, 47(13). https://doi.org/10.1029/2019GL086611

Peace, A., McCaffrey, K., Imber, J., van Hunen, J., Hobbs, R., & Wilson, R. (2018). The role of pre-existing structures during rifting, continental breakup and transform system development, offshore West Greenland. Basin Research, 30(3), 373-394. https://doi.org/10.1111/bre.12257.

Phillips, T. B., & McCaffrey, K. J. (2019). Terrane Boundary Reactivation, Barriers to Lateral Fault Propagation and Reactivated Fabrics: Rifting Across the Median Batholith Zone, Great South Basin, New Zealand. Tectonics, 38(11), 4027-4053. https://doi.org/10.1029/2019TC005772

Rose, I., Buffett, B., & Heister, T. (2017). Stability and accuracy of free surface time integration in viscous flows. Physics of the Earth and Planetary Interiors, 262, 90– 100. https://doi.org/10.1016/j.pepi.2016.11.007

Ryan, J., Frassetto, A. M., Hurd, O., Jones, C. H., Unruh, J., Zandt, G., ... & Owens, T. J. (2020). Unusually deep earthquakes in the central Sierra Nevada (California, USA): Foundering ultramafic lithosphere?. Geosphere, 16(1), 357-377.

Sahoo, T. R., Nicol, A., Browne, G. H., & Strogen, D. P. (2020). Evolution of a normal fault system along eastern Gondwana, New Zealand. Tectonics, 39(10). https://doi.org/10.1029/2020TC006181

Samsu, A., Cruden, A. R., Molnar, N. E., & Weinberg, R. F. (2021). Inheritance of penetrative basement anisotropies by extension-oblique faults: Insights from analogue experiments. Tectonics, 40, e2020TC006596. https://doi.org/10.1029/2020TC006596

Sutton, J., & Watson, J. V. (1986). Architecture of the continental lithosphere. Philosophical Transactions of the Royal Society of London. Series A, Mathematical and Physical Sciences, 317(1539), 5-12.

Thomas, W. A. (2006). Tectonic inheritance at a continental margin. GSA today, 16(2), 4-11. https://doi.org/10.1130/1052-5173(2006)016<4:TIAACM>2.0.CO;2

Thomas, W. A. (2019). Tectonic inheritance at multiple scales during more than two complete Wilson cycles recorded in eastern North America. Geological Society, London, Special Publications, 470(1), 337-352. https://doi.org/10.1144/SP470.4

Vasconcelos, D. L., Bezerra, F. H., Clausen, O. R., Medeiros, W. E., de Castro, D. L., Vital, H., & Barbosa, J. A. (2019). Influence of Precambrian shear zones on the formation of oceanic fracture zones along the continental margin of Brazil. Marine and Petroleum Geology, 101, 322-333. https://doi.org/10.1016/j.marpetgeo.2018.12.010

Wilson, R.W., Klint, K.E.S., Van Gool, J.A.M., McCaffrey, K.J.W., Holdsworth, R.E. & Chalmers, J.A. (2006) Faults and fractures in central West Greenland: onshore expression of continental break-up and sea-floor spreading in the Labrador–Baffin Bay Sea. Geol. Survey Denmark Greenland Bulletin, 11, 185–204.

Wright, L. J., Muirhead, J. D., & Scholz, C. A. (2020). Spatiotemporal Variations in Upper Crustal Extension Across the Different Basement Terranes of the Lake Tanganyika Rift, East Africa. Tectonics, 39(3). https://doi.org/10.1029/2019TC006019